Stability-Oriented Analysis of a DC Shipboard Zonal Distribution System

Andrea Alessia Tavagnutti
Dept. of Engineering and Architecture
University of Trieste
Trieste, Italy
andreaalessia.tavagnutti@phd.units.it

Daniele Bosich
Dept. of Engineering and Architecture
University of Trieste
Trieste, Italy
dbosich@units.it

Giorgio Sulligoi
Dept. of Engineering and Architecture
University of Trieste
Trieste, Italy
gsulligoi@units.it

***Abstract*—The Medium Voltage Direct Current technology and the flexible zonal topology are the enablers to renovate the onboard power use. The several benefits due to DC zonal electrical distributions are possible only in presence of a smart management of the grid. On one side, the tomorrow DC ships must thus rely on a high-performing control, on the other the related large bandwidths can negatively influence the poles positioning of LC filtered systems. Indeed, a not-concurrent design of filters and control system can provide unsuitable solutions, where even a small perturbation can lead to unstable phenomena. To solve this issue, the integrated design procedure is proposed as effective to assure both power quality and stability target. This paper presents an optimized filter design to ensure the DC system stability by taking into account the control requirements. The new stability-oriented method is adopted to conceive the filtering solutions, later verified through eigenvalues analysis and Hardware-In-the-Loop simulations.**

***Index Terms*--DC shipboard power system, stability, filters design, voltage control, control bandwidth, eigenvalues, HIL.**

I. INTRODUCTION

When considering the emissions reduction constraints as well as the will to smartly and efficiently exploit the onboard power resources, the All Electric Ships (AESs) concept represents a must in shipboard power systems [1]. At the same time, the advancement in the power electronics area have also made possible to properly exploit the DC distributions [2]. As the newest vessels are required to be affordable, performing, and reliable, the adoption of the Medium Voltage Direct Current (MVDC) is gaining more and more attention in onboard power grids [3]. In this context, Zonal Electrical Distributions (ZEDS) can be the solution to emphasize these characteristics [4]. A DC distribution enables several benefits in respect to its AC counterpart, like the reduction in overall weight and volume of the power system. Secondly, it is possible to increase the power system flexibility and reliability when adopting a zonal topology [5]. As these technologies are getting an increasing attention in marine applications, innovative solutions and deep investigations are needed to make them exploitable [6]. Great efforts are to be spent to overcome the DC power systems challenges, such as the system-level stability one [7]. The latter is not trivial, as DC power distributions are characterized by a pervasive presence of power converters to interface onboard loads, storage and sources [8]. These converters are coordinated in order to guarantee reconfiguration, protection properties as well as high dynamics performance [4]. Indeed, high control bandwidth are employed to regulate the power system, and the interactions between tightly controlled converters and their LC filtering stages can trigger unstable behaviors. Evidently, the instabilities are to be avoided, while their presence must be foreseen by an accurate stability assessment [3]. Then it is crucial to invest the right attention in the system design process, both on the converters filters and on the control side. In order to prevent instabilities, it is possible to work on the system design stage or to introduce stabilizing signals in the control loops [9]. In this paper the focus will be on the first option.

In complex shipboard microgrid involving multiple power converters, it is useful to identify a practical method to design the filtering stages. To this purpose, a convenient idea wants to simplify the power system with an equivalent reduced model. In this way, it is possible to assess the system stability, while making the design choices on a more manageable system. This approach is proposed in [10], where a design methodology is suggested for two cascade-connected DC-DC converters. In this paper, the same methodology is extended to a complex zonal DC distribution. Such a new integrated design process will be compared to the traditional design based on the only system power quality to highlight some important advantages. To this aim, small signal studies will evaluate the system stability by employing the Eigenvalues Based Method (EBM) [11]. Then, Average Value Models (AVM) and circuital models will be exploited to verify the methodology validity.

II. SHIPBOARD DC ZONAL POWER SYSTEM

The DC zonal grid under study is depicted in Fig.1. The overall generating power of this onboard grid is 8 MW, and the rated DC bus voltage is equal to 1.5 kV. The port and the starboard buses are the main feeders, these can be connected or disconnected thanks to two redundant DC switches. The sources, the battery storage and the loads are all interfaced to the DC feeders by means of power electronics converters. On

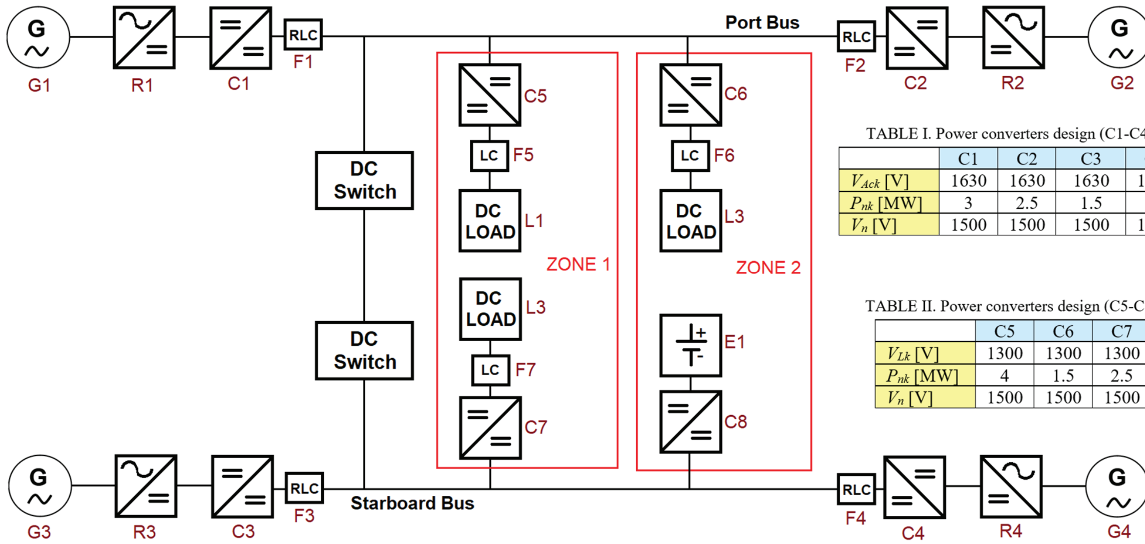

TABLE I. Power converters design (C1-C4).

	C1	C2	C3	C4
V_{Ack} [V]	1630	1630	1630	1630
P_{nk} [MW]	3	2.5	1.5	1
V_n [V]	1500	1500	1500	1500

TABLE II. Power converters design (C5-C7).

	C5	C6	C7
V_{Lk} [V]	1300	1300	1300
P_{nk} [MW]	4	1.5	2.5
V_n [V]	1500	1500	1500

Fig. 1. Zonal electrical DC distribution under study.

the generation side, two of them are on the port side of the ship (G1-G2) and the other ones are on the starboard side (G3-G4). These generating systems are connected to the buses by a cascade of diode-rectifiers (R1-R4) and DC-DC step-down buck converters (C1-C4). Each DC-DC converter is equipped with an LC output filter. To emulate a real onboard distribution, the zonal power system comprises two zones. In the first one two DC loads are included, in the second one there are a DC load and a battery storage. For what concerns the loads, these are supplied by the bus with DC-DC converters (C5-C7). Each converter has its LC output filter (F5-F7), no resistive term is considered in these filters since the losses are assumed to be negligible. The battery pack E1 is interfaced to the starboard bus through a DC-DC buck-boost converter C8, whose filter is not included in Fig. 1 for the sake of simplicity. Since this paper wants to investigate a critical situation, so the converter C8 is disconnected. In such a way, the extra backup power coming from the battery is not available in order to mimic a sort of worst case in terms of stability margins. For all the generating converters, the switching frequency is 1.4 kHz, whereas it is equal to 3 kHz for the load converters. The other characteristics of generating and load converters are included in Table I and Table II, respectively. In particular, the tables provide the following data: converters rated power P_k, rated bus voltage V_n, AC voltage output of the generators V_{ACk} and DC voltage output of the load converters V_{Lk}. A discussion on the converters filters is offered in the next Section instead.

III. Stability-Oriented System Design

The design choices for the generating converters filters are crucial to attain adequate power quality, as well as for ensuring the system stability. Usually, the filters are designed in order to assure a specific voltage $\Delta V_{\%}$, and current $\Delta I_{\%}$ ripple [12]. However, this approach does not take into account the stability issue. In this Section two possible methodologies are suggested for designing the filters of the generating converters. The first one considers just the power quality requirements, whereas the other one takes also into account the stability constraints [10]. Once sized the generating converters filters, the design outputs are to be verified. To this aim, AVM and circuital models are developed as discussed in the last part of this Section.

A. Power quality method

To design the buck converters filters, the first method only takes into account the power quality requirements. This is the most traditional method, and it gives good results if just evaluating the system power quality. The two requirements to be satisfied are the peak-peak voltage ripple $\Delta V_{\%k}$ and the peak-peak current one $\Delta I_{\%k}$. By choosing the first as a target in accordance to the standard [13], the converter filter inductance L_k and capacitance C_k are calculated. The current ripple is not imposed by the standard, while basing on practical experience (i.e. 20-35% is usually adopted). Finally, the resistance value R_k models the converter power losses $\Delta P_{\%k}$, once known the converter rated current I_k. When imposed the converter input voltage U_{nk}, the duty cycle D_{nk} and the switching frequency f_{sk}, eqs. (1) and (2) provide the LC components. The two equations are used for each generating converter and the so-obtained filters data (PQ) are in Table III.

$$\begin{cases} D_{nk} = \dfrac{V_{nk}}{U_{nk}} \\ I_{nk} = \dfrac{P_{nk} - \Delta P_{\%k} \cdot P_{nk}}{V_{nk}} \end{cases} \quad (1) \qquad \begin{cases} R_k = \dfrac{\Delta P_{\%k} \cdot P_{nk}}{I_{nk}^2} \\ L_k = \dfrac{(U_{nk} - V_{nk}) \cdot D_{nk}}{f_{sk} \cdot I_{nk} \cdot \Delta I_{\%k}} \\ C_k = \dfrac{1 - D_{nk}}{8 \cdot L_k \cdot f_{sk}^2 \cdot \Delta V_{\%k}} \end{cases} \quad (2)$$

B. Stability-oriented method

As the first method does not consider the dynamics performance on the loads, a second option is here proposed. The method is the stability-oriented filter design [10], that takes into account both load converters power and control bandwidth ω_k. The data related to the load converters control bandwidths and filters are in Table IV. Before applying the methodology, some hypotheses are to be defined. Firstly, the initial system in Fig. 1

TABLE III. Generating converters filters (C1-C4).

		C1	C2	C3	C4
R_k [mΩ]	-	22.5	27.0	45.0	67.5
L_k [mH]	PQ	0.85	1.0	1.7	2.6
	SO	0.54	0.65	1.1	1.6
C_k [mF]	PQ	1.2	0.99	0.60	0.40
	SO	1.9	1.6	0.94	0.63
$\Delta I_{\%k}$	PQ	20	20	20	20
	SO	32	32	32	32
$\Delta V_{\%k}$	-	2	2	2	2
$\Delta P_{\%k}$	-	3	3	3	3

TABLE IV. Load converters filters and control bandwidths (C5-C7).

	C5	C6	C7
$\Delta V_{\%k}$	3	3	3
$\Delta I_{\%k}$	20	20	20
L_k [µH]	94	250	150
C_k [µF]	657	247	411
ω_k [rad/s]	700	600	500

$$\omega_{f1}^2 = \frac{1}{C_1 \cdot L_1} = \frac{8 \cdot f_{s1}^2}{1 - D_{n1}} \Delta V_{\%1} \quad (3)$$

$$C_1 = \frac{\omega_{2max}}{R^*\left(\omega_{f1}^2 - \omega_{2max}^2\right)} \quad (4)$$

is reduced to a simplified one with a single generating converter and a single load converter. The equivalent load converter power is equal to the total load power while its control bandwidth is the highest among the three load converters, so 700 rad/s. On the other hand, the equivalent generating converter is modeled as a constant voltage source (i.e. fixed duty signal at steady-state) coupled with the Thevenin equivalent of the four LC parallel-connected filters. Once verified that the load converter control bandwidth is sufficiently smaller than its filter bandwidth, the load filter is neglected to obtain a third order model as in [13].

By applying the procedure in [10], the equivalent generating converter filter is thus designed basing on ω_{2max}, the maximum control bandwidth among the load converters. The data regarding the equivalent generating converter are identified with the subscript 1. Once calculated its input filter resonance frequency ω_{f1} (3), and named $R^*=R_L / D_{20}^2$ the overall load resistance moved to the primary, the equivalent capacitance C_1 and inductance L_1 are given by (3)-(4). At this point it is possible to expand this equivalent filter to retrieve the four different generating converters ones (F1-F4), by adopting the equations (2). The latter consider as $\Delta V_{\%}$ the one of the stability-oriented approach (the same as the traditional method) and as $\Delta I_{\%}$ the one that is the result of the design procedure [10].

In Table III, the data of the filters for the two different design methodologies are provided. The letters PQ identify the values from the power quality method, SO the ones from the advanced stability-oriented one. The voltage ripple value is the same for both procedures, nevertheless the current ripple values are different. In the PQ case, the single converters are designed in order to guarantee a $\Delta I_{\%}$ equal to 20% when supplying a resistive load equal to their rated power. In the SO design option this ripple value is equal to 32%, which is still acceptable.

C. Comparison among design procedures

The PQ design method results are apparently valuable, indeed it assures the desired power quality requirements. However, as the stability issue is not considered, this not-wise filters design can potentially drive the system in unstable regions. Conversely, the stability-oriented method SO can give good results both in terms of power quality and stability constraints. Near these two approaches, a third option can design the filters by treating the equivalent load as an ideal CPL [14]. Albeit this method certainly ensures the system stability, the capacitor oversizing determines a troubling increasing in the short circuit current. Only the stability-oriented method can provide an optimized design, where taking into account both power quality requirement and stability constraints, while avoiding oversizing the overall system capacitance.

D. Power system modeling

Three different models are developed to compare the results of the two methodologies and to validate the SO system design. For the preliminary results, two AVM models are implemented on Simulink environment. Then, the validation is assigned to a detailed circuital real-time simulator: in such a case, the Typhoon HIL 604 is the adopted platform. The system under study is the one in Fig.1. Here, the DC switches are closed while the converter C8 is disconnected to simulate a condition in which the battery does not perform the bus voltage support function. Then, all the generating converters are droop controlled to participate in the voltage regulation.

The AVM models of each generating and load converter are implemented as in [11]. The first complete model is thus a simplified AVM in which the load converters filters are neglected as in the SO design procedure. This simplified model is employed to assess the power system small-signal stability, for the two system design procedures (i.e. PQ and SO). The stability assessment is performed by adopting the EBM method [11]. After verifying that only the SO methodology ensures a stable evolution, the related dynamic transients are given. Then, another AVM model is consequently built to also include the load converters filters. In such a way, it is possible to verify the considerations made on the simplified model.

The last step is the implementation of the DC zonal distribution in a circuital simulator. Thereby, the switching behavior of the converters is included while their controlled operation is accurately modeled. To properly exploit this platform, the power system is organized in order to use 3 cores, in this way the sampling time is equal to 0.5 µs. In the next Section, not only the stability assessment is reported but also the results of Simulink simulations and Typhoon emulations.

IV. Results

The previously defined models are now exploited to compare the two design choices in terms of small signal stability. Such an evaluation is highlighted both in poles positioning and in transient responses. The system under analysis is in steady-state condition. The C6-C7 converters feed the loads with their rated power, while the C5 converter supplies the 90% of its rated power. This load is the most demanding, since it has both largest rated power and highest control bandwidth. At 1 s, a small perturbation is applied to the system by adding the last 10% to the C5 load request.

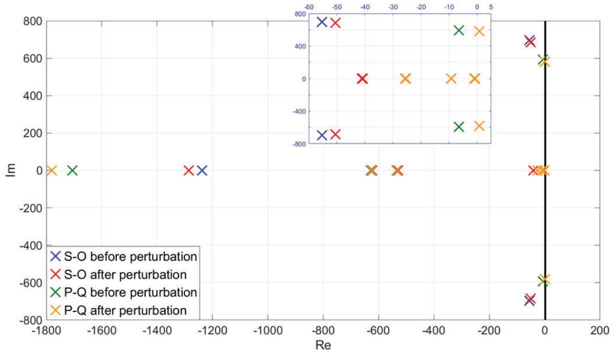

Fig. 2. System poles location.

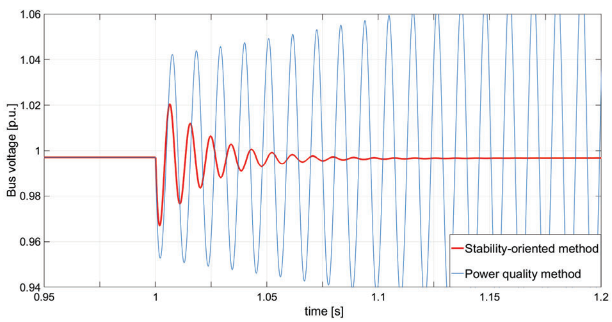

Fig. 3. Simplified AVM transient response (Simulink).

A. *Stability assessment*

Once neglected the load converters filters, the simplified AVM is adopted to study the small-signal stability. The methodology of [11] is then applied by linearizing the system differential equations around the operating points, both for the system before and after the perturbation. When the linearized systems' matrices are defined, the eigenvalues can be calculated for both PQ-SO designed filters. The results are in Fig. 2, where each color represents a specific designed methodology in a specific condition. The poles at which is given attention are the complex conjugate ones, since these are the ones that can move in the right half plane, so in the unstable position. As the poles of the system designed with the SO method are sufficiently far from the imaginary axis both before and after the perturbation, a stable evolution is foreseen. Whereas the poles of system designed following the PQ method are close to the stability boundary (black line) before the perturbation. By increasing the load in the most demanding converter (+10%), the system poles shift on the right half plane, thus an unstable evolution is predicted. The information coming from the poles analysis are also confirmed by the transient responses of nonlinear simplified AVM models in Fig. 3. Here, the response after the perturbation is shown for both the system designed by PQ-SO methods. When the L1 load is increased to its rated power, an unstable behavior is triggered in the system previously designed by PQ approach. Conversely, the system designed with SO method presents a stable evolution. The design on generating converters filters is made on the system in which the load filters are neglected. In the next subsection, the simulations performed on the complete AVM and on the HIL circuital model will confirm the relevant results here revealed.

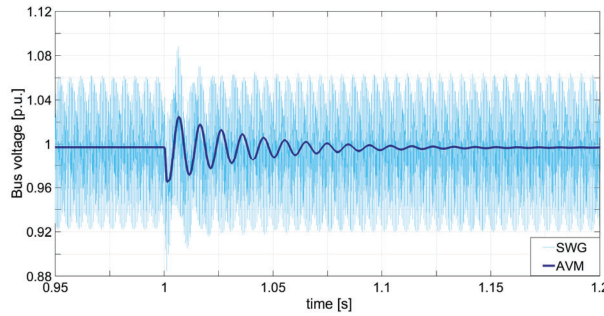

Fig. 4. Bus voltage transient,
AVM (Simulink) and circuital model (Typhoon HIL).

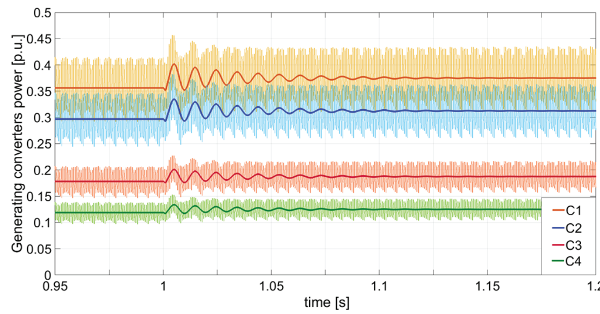

Fig. 5. Generating converter power transient,
AVM (Simulink) and circuital model (Typhoon HIL).

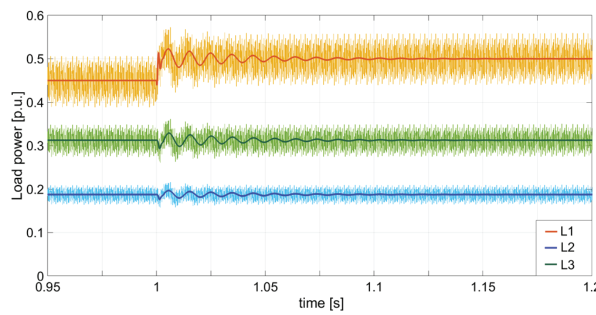

Fig. 6. Load converter power transient,
AVM (Simulink) and circuital model (Typhoon HIL).

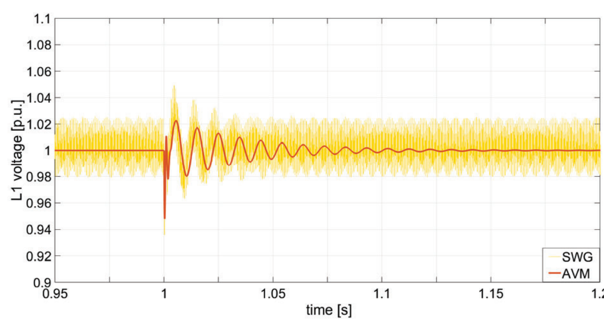

Fig. 7. L1 voltage transient,
AVM (Simulink) and circuital model (Typhoon HIL).

B. *Transient response*

The stability assessment is performed on a simplified model of the system. The complete model of the power distribution is here employed to finally check the results by a numerical confirmation. The results included in this Subs. are related to the stable system, so the one designed with the SO procedure. For the power transients, the results are in per unit of the total generating rated power. The rated bus and load voltage are the basis for the voltage transients. In the transients figures, both the results of Simulink and Typhoon simulations are highlighted. This comparison among platforms is done to additionally verify that an accurate AVM model is sufficient to define the DC system behavior for the stability purposes.

Before the perturbation the system is at steady state, the generating converter are supplying the loads with a power of 7.6 MW. The loads L2 and L3 require their rated power, whereas the most demanding load L1 requires 90% of its one. Previous studies predict a stable evolution after the perturbation. This is confirmed both by the AVM and the switching Typhoon HIL results. In all the figures, bold lines are used to depict the AVM transient and thin lines for the switching one. In the bus voltage transient of Fig. 4, the stability is maintained and after some oscillations the voltage settles in approximately 100 ms. The voltage value at steady state is not equal to 1 p.u. because of the droop effect. Thanks to the droop signal, the decoupling between the converters is ensured, while at the same time it is possible to control the power sharing ratio between the generating converters. In this work, the sharing choice is to set the droop gain in reasons of the converters rated powers. This is visible in Fig. 5, where C1-C4 output power are shown. Before the perturbation, each converter output is equal to the 95% of their rated power. When the perturbation occurs, the converters are forced to feed the loads with their entire rated power. In Fig. 6, the load converters output powers are provided. Here the load increase in the L1 load is shown, indeed at 1 s it increases from 3.6 MW to 4 MW. Finally, Fig. 7 highlights the voltage dynamics response of C5, the highest performance converter which supplies the most demanding load.

The important results of this paper are useful to emphasize the validity of the stability-oriented methodology. As highlighted in the eigenvalues analysis, the system designed just considering the power quality requirements presents an unstable behavior. Whereas the one designed with the SO methodology is characterized by a stable evolution. At the same time, this second methodology still guarantees the desired voltage ripple (i.e. the most strict requirement) and at the same time it does not oversize the filter capacitance. The correspondence between AVM and switching transients finally proves that simplified model can be powerful also when increasing the power system's complexity as in the zonal case.

V. CONCLUSIONS

This paper has discussed about the system stability issue on shipboard MVDC zonal electrical distributions. To design the LC filters, the stability-oriented design methodology has been conceived and then compared to a more standard approach. Thanks to the eigenvalue analysis, the instability arise has been predicted in the traditionally designed system, while the new design method has sized a system with lager stability margins. Several models have been developed to assess the system stability, then validating the new design procedure. A complex circuital model in a real-time HIL emulator not only has been useful to understand the power system's real behavior, but also it has provided a final verification on simplified models. Indeed, the comparison between AVM and switching transients has finally testified the effectiveness of AVM modeling. The possibility to analyze a complex system by means of reduced order models has been therefore confirmed.

ACKNOWLEDGMENT

The authors would like to thank Typhoon HIL for providing the HIL platform used in the development of this research work.

REFERENCES

[1] S. Fang, Y. Wang, B. Gou and Y. Xu, "Toward Future Green Maritime Transportation: An Overview of Seaport Microgrids and All-Electric Ships," in *IEEE Transactions on Vehicular Technology*, vol. 69, no. 1, pp. 207-219, Jan. 2020.

[2] F. Wang, Z. Zhang, T. Ericsen, R. Raju, R. Burgos and D. Boroyevich, "Advances in Power Conversion and Drives for Shipboard Systems," in *Proceedings of the IEEE*, vol. 103, no. 12, pp. 2285-2311, Dec. 2015.

[3] "IEEE Recommended Practice for 1 kV to 35 kV Medium-Voltage DC Power Systems on Ships," in *IEEE Std 1709-2018 (Revision of IEEE Std 1709-2010)* , vol., no., pp.1-54, 7 Dec. 2018.

[4] G. Sulligoi, D. Bosich, A. Vicenzutti and Y. Khersonsky, "Design of Zonal Electrical Distribution Systems for Ships and Oil Platforms: Control Systems and Protections," in *IEEE Transactions on Industry Applications*, vol. 56, no. 5, pp. 5656-5669, Sept.-Oct. 2020.

[5] J. G. Ciezki and R. W. Ashton, "A technology overview for a proposed navy surface combatant dc zonal electric distribution system," *Naval Engineers Journal*, vol. 111, no. 3, pp. 59–69, 1999.

[6] M. E. Baran and N. R. Mahajan, "DC distribution for industrial systems: opportunities and challenges," in *IEEE Transactions on Industry Applications*, vol. 39, no. 6, pp. 1596-1601, Nov.-Dec. 2003.

[7] U. Javaid, F. D. Freijedo, W. van der Merwe and D. Dujic, "Stability Analysis of Multi-Port MVDC Distribution Networks for All-Electric Ships," in *IEEE Journal of Emerging and Selected Topics in Power Electronics*, vol. 8, no. 2, pp. 1164-1177, June 2020.

[8] J. Siegers and E. Santi, "Stability analysis and control design for an all-electric ship MVDC power distribution system using a passivity based stability criterion and power hardware-in-the-loop simulation," *Proc. 2015 IEEE Electric Ship Techn. Symposium (ESTS)*, 2015, pp. 86-92.

[9] A. Riccobono and E. Santi, "Comprehensive Review of Stability Criteria for DC Power Distribution Systems," in *IEEE Transactions on Industry Applications*, vol. 50, no. 5, pp. 3525-3535, Sept.-Oct. 2014.

[10] D. Bosich and G. Sulligoi, "Stability-Oriented Filter Design optimization in Cascade-Connected MVDC Shipboard Power System," *Proc. 2020 IEEE Power & Energy Society Gen. Meeting (PESGM)*, 2020, pp. 1-5.

[11] A. A. Tavagnutti, D. Bosich and G. Sulligoi, "A Multi-Model Methodology for Stability Assessment of Complex DC Microgrids," *Proc. 2021 IEEE Fourth International Conference on DC Microgrids (ICDCM)*, 2021, pp. 1-7.

[12] M. B. El Kattel, R. Mayer, M. D. Possamai and S. Vidal Garcia Oliveira, "A Simplified Analysis of Buck-Type Interleaved DC-DC Converter for Battery Chargers Application," *2019 IEEE 15th Brazilian Power Electronics Conference and 5th IEEE Southern Power Electronics Conference (COBEP/SPEC)*, 2019, pp. 1-6.

[13] S. Pastore, D. Bosich and G. Sulligoi, "Analysis of small-signal voltage stability for a reduced-order cascade-connected MVDC power system," *Proc. IECON 2017 - 43rd Annual Conference of the IEEE Industrial Electronics Society*, 2017, pp. 6771-6776.

[14] M. Cupelli, L. Zhu and A. Monti, "Why Ideal Constant Power Loads Are Not the Worst Case Condition From a Control Standpoint," in *IEEE Transactions on Smart Grid*, vol. 6, no. 6, pp. 2596-2606, Nov. 2015.